Large visual neuron assemblies receptive fields estimation using a super-resolution approach

Daniela Pamplona, Gerrit Hilgen, Matthias H. Hennig, Bruno Cessac, Evelyne Sernagor, Pierre Kornprobst

Large visual neuron assemblies receptive fields estimation using a super resolution approach

Daniela Pamplona, Gerrit Hilgen, Matthias H. Hennig, Bruno Cessac, Evelyne Sernagor, Pierre Kornprobst

RESEARCH REPORT
N° 9383
December 2020
Project-Team Biovision

ISSN 0249-6399 ISRN INRIA/RR--9383--FR+ENG

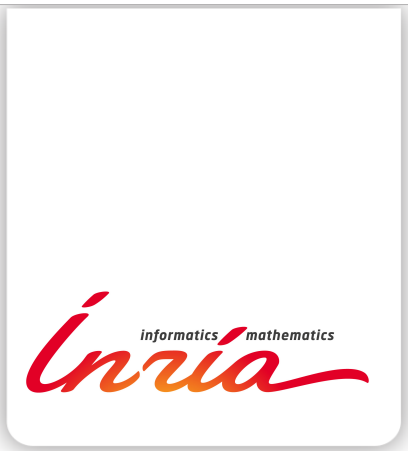

Large visual neuron assemblies receptive fields estimation using a super resolution approach

Daniela Pamplona[*†], Gerrit Hilgen[‡], Matthias H. Hennig[§], Bruno Cessac[*], Evelyne Sernagor[‡], Pierre Kornprobst[*]

Project-Team Biovision

Research Report n° 9383 — December 2020 — 23 pages

This work was partially supported by the EC IP project FP7-ICT-2011-9 no. 600847 (RENVISION)

[*] Université Côte d'Azur, Inria, France
[†] Ecole Nationale Supérieure de Techniques Avancées, Institut Polytechnique de Paris, U2IS, 828 Boulevard des Marchaux, 91120 Palaiseau, France
[‡] Institute of Neuroscience, Faculty of Medical Sciences, Framlington Place, Newcastle upon Tyne, NE2 4HH, United Kingdom
[§] Institute for Adaptive and Neural Computation, School of Informatics, University of Edinburgh, 10 Crichton Street, Edinburgh, EH8 9AB, United Kingdom

RESEARCH CENTRE
SOPHIA ANTIPOLIS – MÉDITERRANÉE

2004 route des Lucioles - BP 93
06902 Sophia Antipolis Cedex

Abstract: One primary goal in analyzing sensory neurons' recordings is to map the sensory space to the neural response, thus estimating the neuron's receptive fields (RFs). For visual neurons, the classical method to estimate RFs is the Spike Triggered Average (STA). In short, STA consists estimate the average stimulus before each spike evoked by a white noise stimulus whose block size can be ad-hoc tuned to target one single neuron. However, this approach becomes impractical to deal with in large scale recordings of heterogeneous populations of neurons since no single block size can match all neurons. Here, we aim to overcome this limitation by leveraging super resolution techniques to extend STA's scope. We defined a novel type of stimulus, the shifted white noise, by introducing random spatial shifts in the white noise stimulus. We evaluated this new stimulus thoroughly on both synthetic and real neuronal populations of size 216 and 4798, respectively. Considering the same target STA resolution, results across the population with synthetic case show that the average error using our stimulus was 1.7 times smaller than the error using the classical stimulus. We could map 2.3 times more neurons and cover a broader heterogeneity of RF sizes. For a single neuron, we show how it can be mapped after only one minute of stimulation, while after 11 minutes, this neuron was still not mapped with the classical one, which emphasizes the effectiveness of our method. Analogously, similar results were obtained with real neurons' experiment. Considering the same target STA resolution, we mapped 18 times more RFs and we found a broader heterogeneity of RFs sizes (the kurtosis of the distribution of the RF sizes is 0.3 times smaller). Overall, the shifted white noise improves the RFs' estimation in several ways. Our approach performs better at the single-cell level. RF estimation is independent of the neuron's position relative to the stimulus and offers high-resolution. Our approach is stronger at the population-level. We get more RF with more neuronal variability. Our approach is faster, enabling experimentalists to get results in shorter stimulation time. Furthermore, this stimulus can also be used in other spike-triggered methods, extended to the time dimension, and adapted to other sensory modalities. Due to its design simplicity and strong results, we expect that soon the shifted white noise is used as a rule and allows revealing novelties in sensory analysis.

Key-words: Receptive fields, sensory neurons, Spike Triggered Average, super-resolution, retina

Estimation des champs récepteurs de grands ensembles de neurones visuels par une approche de super-résolution

Résumé :

L'un des principaux objectifs de l'analyse des enregistrements des neurones sensoriels est de faire correspondre l'espace sensoriel à la réponse neurale, ce qui permet d'estimer les champs récepteurs (RF) des neurones. Pour les neurones visuels, la méthode classique d'estimation des RF est le Spike Triggered Average (STA). En bref, STA consiste à estimer le stimulus moyen avant chaque impulsion évoquée par un stimulus de bruit blanc dont la taille du bloc peut être réglée ad hoc pour cibler un seul neurone. Cependant, cette approche devient peu pratique pour les enregistrements à grande échelle de populations hétérogènes de neurones, car aucune taille de bloc ne peut correspondre à tous les neurones. Ici, nous cherchons à surmonter cette limitation en tirant parti des techniques de résolution pour étendre le champ d'application du STA. Nous avons défini un nouveau type de stimulus, le bruit blanc décalé, en introduisant des décalages spatiaux aléatoires dans le stimulus du bruit blanc. Nous avons évalué ce nouveau stimulus de manière approfondie sur des populations neuronales synthétiques et réelles de taille 216 et 4798, respectivement. En considérant la même résolution STA cible, les résultats sur la population synthétique montrent que l'erreur moyenne utilisant notre stimulus était 1.7 fois plus petite que l'erreur utilisant le stimulus classique plus petit. Nous avons pu identifier 2.3 fois plus de neurones et couvrir une plus grande hétérogénéité de tailles de RF. Pour un seul neurone, nous avons montré comment il peut être identifié après seulement une minute de stimulation, alors qu'après 11 minutes, ce neurone n'était toujours pas identifié avec le stimulus classique, ce qui souligne l'efficacité de notre méthode. De même, des résultats similaires ont été obtenus avec l'expérience sur des neurones réels. En considérant la même résolution de STA cible, nous avons identifié 18 fois plus de RF et nous avons trouvé une plus grande hétérogénéité des tailles de RF (l'aplatissement de la distribution des tailles de RF est 0.3 fois plus petit). Dans l'ensemble, le bruit blanc décalé améliore donc l'estimation des RF de plusieurs façons. Notre approche est plus performante au niveau d'une seule cellule. L'estimation des RF est indépendante de la position du neurone par rapport au stimulus et offre une haute résolution. Notre approche est plus performante au niveau de la population. Nous obtenons plus de RF avec une plus grande variabilité neuronale. Notre approche est plus rapide, ce qui permet aux expérimentateurs d'obtenir des résultats en un temps de stimulation réduit. En outre, ce stimulus peut également être utilisé dans d'autres méthodes déclenchées par des impulsions, étendues à la dimension temporelle et adaptées à d'autres modalités sensorielles. En raison de la simplicité de sa conception et de ses bons résultats, nous espérons que le bruit blanc décalé sera bientôt utilisé comme règle et qu'il permettra de révéler des nouveautés en matière d'analyse sensorielle.

Mots-clés : Champs récepteurs, neurones sensoriels, Spike Triggered Average, super-résolution, rétine

1 Introduction

Sensory neurons are characterised by their receptive field (RF), which is the size of the sensory space they respond to upon stimulation. In the case of visual neurons, it is the area of the visual field these cells respond to when light intensity changes in that space. To estimate the size and shape of an RF with high accuracy, it is imperative to take the measurements at sufficiently high spatial resolution. Ideally, high fidelity RF measurements should consist of sampling at very high resolution, which means stimulating small subunits (pixels) of the RF in sequence. However, when these pixels are too small, it becomes challenging to elicit a neural response, as normally, cells respond to simultaneous stimulation of many pixels in their RF. On the other hand, when the pixel size is too large, responses do not reflect RF sizes faithfully, and differences between RFs of adjacent cells may be blurred. This problem is exacerbated by the fact that RF sizes are not homogeneous across the neuronal population. Retinal ganglion cells (RGCs), for example, have smaller RFs in the centre of the retina than in the periphery, hence the optimal pixel size to determine central RFs is smaller than for measurements in the periphery. Owing to new technological developments in recording approaches consisting of large-scale, high-density multielectrode arrays (MEAs), it is now possible to record responses to light from hundreds to thousands of neurons simultaneously [2], encompassing both central and peripheral cells. Such an experimental scenario requires to design new stimuli that can yield high-resolution measurements for all cells across the neural population.

In this study, we present a novel approach to measure RFs at high fidelity from large and heterogeneous neural populations recorded simultaneously. The classical way of estimating RFs is to estimate the Spike Triggered Average (STA) from evoked neural recordings. In short, Spike Triggered Average (STA) consists estimate the average stimulus before a spike. If the stimulus is white noise, then under the Linear-Nonlinear Poisson (LNP) neural model, this average is proportional to neuron Receptive Field (RF) [20, 9]. White noise consists of a series of non-overlapping binary images shown successively in time, with individual images showing a black or white pixel of similar size presented in random order but with equal probability. Let us call this stimulus Black White Noise (BWN). BWN has two advantages. It has high contrast between blocks, which is optimal to elicit strong responses in the retina or the lateral geniculate nucleus (LGN) of the thalamus. Technically, it is easy to generate because the only parameter to choose from is the size of the blocks.

In the case of single-cell recordings, the block size is defined based on the experimenter's expectations: it must be smaller than the expected RF size to have a high resolution on the estimated RF, but it cannot be too small to avoid low rate neural responses. There exist methods to solve this problem in a less heuristic way. For instance, one can start from a tiny block size and increase it during the experiment in the direction of the larger stimulus-neural response correlation [8] or mutual information [14, 15]. However, in the case of large populations of neurons, one cannot merely apply the same procedure as in the single-cell case. Indeed, a "good" block size for one neuron will be "bad" for another one in the population. Similarly, a high stimulus-neural response correlation (or mutual information) for one neuron might mean low for another one. As a consequence, experimenters have to find a size that best suits the population as a whole. This approach effectiveness will thus strongly depend on the neuron population degree of heterogeneity.

Here we use a novel white noise stimulus, which we call Shifted White Noise (SWN). The size of each block is large, ensuring strong responses from all RGCs. However here, the blocks are shifted only by a fraction of their size, yielding high-resolution sampling. In other words, large pixels ensure strong light responses while sub-pixel shifts yield super-resolution measurements, enabling us to measure all RFs with great accuracy. Super-resolution is a class of image

processing methods to estimate a high-resolution image from a set of low-resolution ones [28]. Super-resolution has been successfully applied to a variety of domains such as, e.g., video [13], remote sensing [27, 17], and medical imagery [10, 22]. Interestingly, even if we are not in the case of a pure image reconstruction problem, we found exciting analogies with our problem here. In a nutshell, to increase the resolution of RF, the idea is not to diminish the block size (which would end up with less responsiveness of the cell and thus a wrong RF estimation), but instead, keep a high block size while introducing and additional spatial variability in the stimulus to excite more optimally the cells. Here is our method's central ability: Make the majority of cells more responsive to let us find RF more rapidly and accurately, which then answers the three main objectives stated above.

This paper is organised as follows. In Section 2, we motivate and define our new class of stimuli, called Shifted White Noise (SWN). In Section 3, we consider an artificial neuron population to show the performance of our approach on a fully controlled case, i.e., with synthetic data. Our case-study focuses on retina-like neuron models. We define a parametrised population of 216 neurons to ensure heterogeneity. The fact that ground-truth is known enables us to carefully evaluate our approach compared to the baseline, i.e., Basic White Noise (BWN). In Section 4, we then consider real data, namely a population of 4978 ganglion cells of a mouse recorded from a multielectrode array (with 4096 microelectrodes). Finally, in Section 5, we discuss potential avenues for future research.

2 A new class of visual stimuli

This section proposes a new class of visual stimuli that could be used to estimate Receptive Field (RF) using Spike Triggered Average (STA). However, to use STA, one needs some constraints on the stimulus. What theory says is that, in order for the STA converge to the RF, the stimulus must be white or, at least, possibly radially symmetric by matrix multiplication [20].

The typical stimulus is illustrated in Fig. 1 (A). We call it here BWN. It consists of a sequence of binary images showing equal-sized blocks, with a color drew randomly from a Bernoulli distribution with a probability 0.5. Each image is displayed during a fixed time to the visual neurons. Since STA relies on averaging stimuli within time-windows, it is interesting to note that the resulting spatial precision of the estimated RF is equal to the block's size from the BWN. This spatial precision will also be called resolution in the sequel. As a consequence, a natural idea to increase the resolution of the receptive fields would be to lower the block size of the BWN, as shown in Fig. 1 (B). Unfortunately, such a solution will not work in general. By diminishing block size too much (considering a given neuron), the classical side-effect is to diminish the spiking response of the neuron. Having fewer spikes, STA approach becomes less efficient since it would require much more extended recording periods to map RFs.

Here comes the idea of super-resolution. Since it is crucial to preserve large block sizes to guarantee responsiveness, another option is to present a similar series of binary images but with a given random shift in space. Two such examples are shown in Fig. 1 (C–D). Apparently, this does not change much the situation since, for each condition, one obtains a low-resolution RF. However, having all these low-resolution estimates with various shifts, one can imagine combining them to get a high-resolution RF. This problem is a super-resolution problem by definition, i.e., we have to estimate a high-resolution image from a variety of low-resolution samplings.

Thus a possible strategy could be defined as follow. Let us denote by β the block size of the stimuli, and define the target resolution for the RF as $\alpha = \beta/k$ (e.g., $k = 2$ means that we want to double the resolution). This target resolution defines a baseline shift (of the same value) from which one can define a series of random spatial shifts $s = n\alpha$ with $n \in \{0, \ldots, k-1\}$. Considering

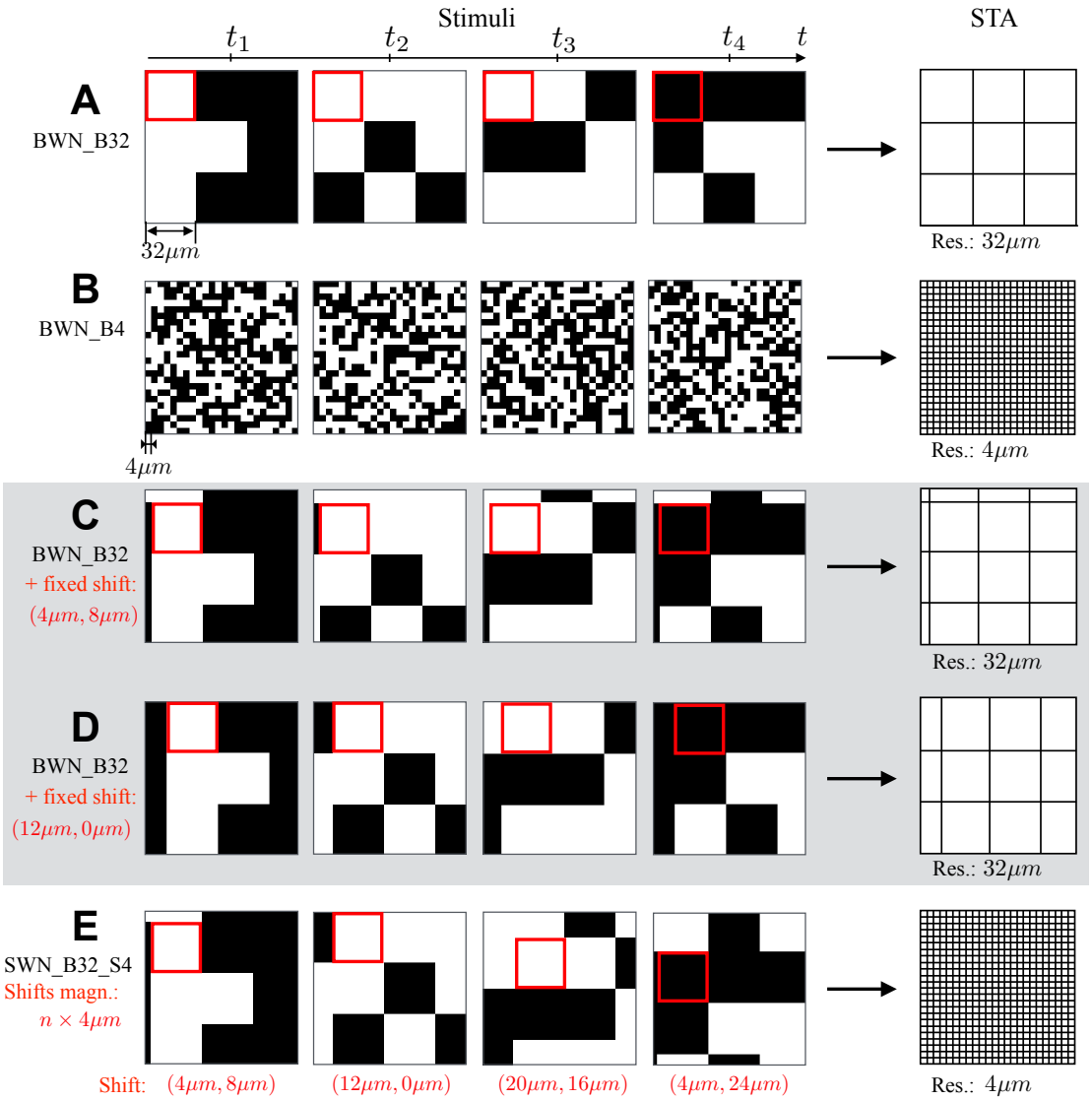

Figure 1: Exploring variation across white noise stimuli: From Basic White Noise (BWN) to Shifted White Noise (SWN). (A) BWN_B32: Basic White Noise (BWN) with blocks of 32 µm. In the BWN case, the resolution of the RF is the same as the size of the blocks. (B) BWN_B4: same as (A) but with blocks of isze 4 µm. (C) and (D): Series of BWN_B32-like stimuli based on example (A), with an additional fixed spatial shift. The spatial shift is represented by a red square showing how the upper-left block has been moved. The resolution of the STA is still the same as the size of the blocks. However, the different shifts will infer different samplings of the RF that could be combined to achieve a high-resolution RF (see text for details). Note that starting from (A) was chosen only for explanatory purposes so that readers could compare both conditions. The binary patterns should be a priori random. (E) Shifted White Noise (SWN)-B32-S4: Shifted White Noise (SWN) with blocks of 32 µm and random spatial shifts using a baseline shift of 4 µm. With this condition, it is the baseline shift that defines the resolution of the RF.

blocks of standard BWN images, the idea is to apply to each block one of the shifts. Altogether, the whole stimulus would consist of a succession of blocks characterized by the same shift. Using the STA for each block would provide one RF per block, and then, one could combine them to get a high-resolution RF (e.g., think about a simple average between all these estimations).

The method we propose is based on this notion of random shifts. However, instead of applying the STA for each block, our idea is to randomize the different conditions (shifts) entirely and apply the STA globally. The sequence of images obtained in this way is what we call Shifted White Noise (SWN). It is illustrated in Fig. 1(E).[1] Compared to the strategy described above, using SWN has two main advantages. First, the high-resolution RF directly results from the STA. There is no need to estimate intermediary low-resolution RF and then combine them in some way. Second, by randomizing conditions, we can introduce more variability for the overall population of neurons. More variability means more responsiveness and less experimental time devoted to that task, which is our goal.

In summary, SWN brings many advantages with respect to the traditional BWN. While the resolution of the RF is given by the block size with BWN, it is independent of block size with SWN. With SWN, it is only given by the baseline shift, which will let the experimenter choose a sufficiently large block size to favor neuron responsiveness. Given this, one can achieve a very high resolution where the only limitation will come from the experimental setup (i.e., size of the projected pixel of the light stimulation equipment). Another significant advantage of SWN is that it introduces more variability, favoring better light response across the overall population. So, we expect to obtain RF of high-resolutions, but we also expect to find more RF and in shorter stimulation periods. These are the three properties of SWN that will be studied in the next two sections, considering synthetic and real data.

From now on, in this paper, the stimuli are named as follows:

- A Basic White Noise (BWN) with a block size β will be denoted by BWN-Bβ.
- A Shifted White Noise (SWN) with a block size β and a baseline shift α will be denoted by SWN-Bβ-Sα.

All sizes are expressed in μm.

3 Performance analysis on synthetic data

This section analyzes the impact of the stimulus on Receptive Field (RF) estimation using an artificial population of Linear-Nonlinear Poisson (LNP). Considering a synthetic case provides the following benefits: (1) The model assumption is valid, and therefore the Spike Triggered Average (STA) convergence only depends on the stimulus [20], (2) The STA error can be estimated by directly comparing the ground truth RF with the STA, (3) the error evolution over time can be compared with the theoretical expectations [20], and (4) One can fit STA result with the same model function that generated the RF, and the resulting parameters can be compared with the ground truth ones. In Section 3.1, we present the neuron model, how a population is defined, how they are stimulated, and finally, how results will be analyzed. In Section 3.2, we show the performance of our approach at both single-cell and population levels.

[1] Code to generate stimuli will be provided upon acceptance of the paper

3.1 Methods

3.1.1 Stimuli

In the experimental analysis we consider three stimuli: two Basic White Noises (BWNs) of low and high resolution (32 µm and 4 µm, respectively) and one Shifted White Noises (SWNs) whose STA is of resolution 4 µm (with blocks of 160 µm and shifts of 4 µm).

For each stimulus we generated 27K images of 88×88 pixels, where one pixel corresponds to a square of size $4\,\mu\text{m})^2$). Here we arbitrarily set the origin at the central pixel of the spatial domain, which will be more convenient to specify neurons' population. Images were refreshed at 30.3Hz meaning, each image was showed for 33 ms.

Each stimulus will be fed independently to our artificial population of neurons described below to obtain the simulated spiking output and then the RF estimation using STA. Each image will be presented for 1ms corresponding to one discrete time-step in our model.

3.1.2 Artificial retinal Ganglion cell model

In this work, we define a population of neurons described by LNP models [19, 6]. These functional models are widely used by experimentalists to characterize the cells that they record, map their receptive field, and characterize their spatio-temporal feature selectivities [12, 7, 4, 25, 1]. It can be shown that the STA of a LNP neuron stimulated with random white noise converges to the RF of the neuron, up to a multiplicative constant [20].

In its simplest form, a LNP model is a convolution of the stimulus L with a spatio-temporal kernel K followed by a static non-linearity and stochastic (Poisson-like) mechanisms of spikes generation. Here we use this model to simulate retinal ganglion cells' spiking activity in response to our stimuli. The detailed definition is given in the Appendix (see Sec. 6.1).

3.1.3 Neural population construction

Given the neuron's model described in Section 3.1.2, our goal is to define an heteregenous population of such neurons that will cover the different scenarios expected in real experiments. The heterogeneity will come from the choice of the parameters in the spatial part of kernel K (see (3)), namely the center of the RF denoted by (c_x, c_y) and the size of the central RF given by σ_c

The generation process is illustrated in Fig. 2. First, we choose as a reference grid the grid provided by the BWNs of low resolution, i.e., with blocks of size 32 µm. The idea is to define a population of neurons where we vary positions and kernel sizes. More precisely, we define a population of 216 neurons as follows:

- We first define a set of positions. Starting from position $c_0 = (0, 0)$ (at the center of the spatial domain), we define a family of neurons equally sampled along the diagonal direction in steps of one pixel ($\delta_c = 4\,\mu\text{m}$) until the next block center c_{max} (see Fig. 2(A)). Doing so, we define nine positions:

$$(c_x, c_y) = \{(0, 0), (\delta_c, \delta_c), \ldots, (8\delta_c, 8\delta_c)\} = \{(0, 0), (4, 4), \ldots, (32, 32)\}.$$

  Note that one parameter is sufficient to describe neuron position, namely we use c_x in the remaining part of this paper.

- Then, for each neuron position, we define a family of neurons with varying spatial kernel sizes (see Eq. (3)). The smallest radius r_0 corresponds to a center standard deviation $\delta_\sigma = 0.784\,\mu\text{m}$. In this way, the size of the center Gaussian (the circumference radius where the Difference of Gaussian (DOG) changes from positive to negative) is 2 µm. The

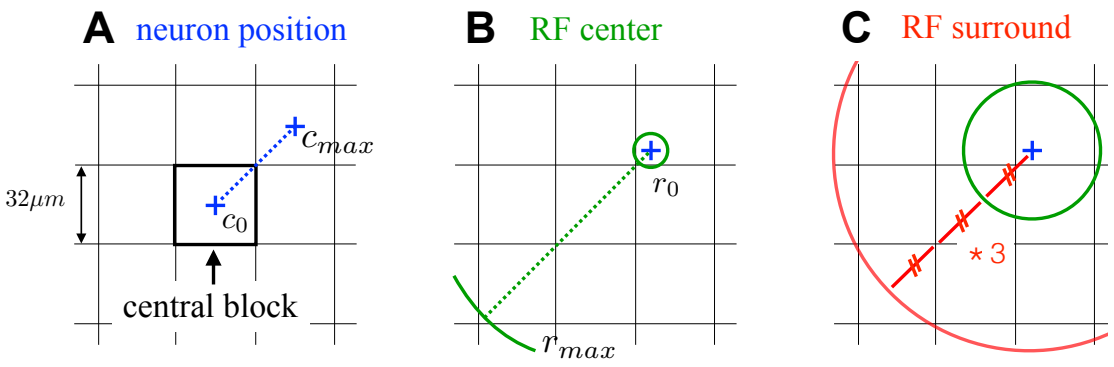

Figure 2: Stages to build the artificial retinal Ganglion population. (A) We define nine positions equally distributed between the center of the central block (c_0) and the center of the adjacent block in the diagonal direction (c_M). (B) For the spatial kernel, we define 24 possible values of σ_c, so that the positive part radius vary from half pixel to 1.5 blocks in steps of half pixel. The smallest RF have radius of 2 µm and the largest 24 µm. (C) We assume here that the surround variance to three times the center variance.

remaining σ_c were defined as a multiple of this one, increasing in steps of 2 µm (meaning, half pixel) the center radius (see Fig. 2(B)). Doing so, we defined 24 possible values of σ_c:

$$\sigma_c = \{\delta_\sigma, 2\delta_\sigma, \ldots, 24\delta_\sigma\} = \{0.784, 1.568, \ldots, 18.824\}.$$

Concerning the surround standard deviation, σ_s, it was set to three times σ_c as usually fixed in the literature (see Fig. 2(C)). Thus only one parameter is sufficient to describe the spatial kernel amplitude, i.e., σ_c.

3.1.4 Spike Triggered Average (STA)

The STA is a reverse-correlation technique commonly used to estimate the RF of neurons that relies on both neuron model and stimulus properties [4, 25, 20, 9]. The STA corresponds to the average sequence of images preceding spikes. It is defined as follows. Consider a neuron (model or experimental) that spiked at times $t_1, t_2, \ldots, t_n$ when stimulated by a spatio-temporal stimulus $S(x, y, t)$, then the STA of this neuron, denoted by $A(x, y, \tau)$, is given by:

$$A(x, y, \tau) = \frac{1}{n} \sum_{i=1}^{n} S(x, y, t_i - \tau),$$

with x and y belong to the same spatial domain as the stimulus S and τ is on $\{-\mathcal{T} \ldots 0\}$ where $-\mathcal{T}$ defines the temporal support of the STA.

STA allows a parameter free estimation of the RF, it is easy to design and use experimentally in any biological sensory modality.

To estimate the STA, we use the PRANAS, an open and free platform for retinal analysis and simulation [3].

3.1.5 Evaluation

We propose three criteria to evaluate the assess the validity of the SWN.

Criterion 1 (Number of mapped RFs) We consider that a RF was mapped if the STA 2D spatial profile was structured, thus if there is a blob, or a point where non zeros values are concentrated. To recess automatically whether a RF was mapped or not, we made a Student's T-test with a significance level $\alpha = 1e^{-8}$ on the 2D-spatial profile of each STA. If the 2D-spatial profile is Gaussian distributed, thus if it is noise, then then RF was not mapped. Otherwise, we considered that the RF was mapped.

Criterion 2 (RF parametric description) For a mapped RF, we propose to fit the spatial RF with a DOG as defined in eqn. (3). For that, we used the Trust Region Reflective method [18, 16], which is a bounded minimization algorithm. In practice, in order to balance between parameters variability and algorithm efficiency, we defined large bounds for each parameter: σ_c lower value is 0.1 and higher value is three times the image size in µm; c_x and c_y lower value is equal to 1 µm and higher value the image length. To avoid local minima each STA was fitted 12 times with different initializations uniformly sampled within the bounds. Then, for the analysis, we selected the parameters that minimize the fitting error.

Criterion 3 (STA error) In the synthetic case, we can compare the STAs with the GTs "point-by-point". To do so, we measure the angle between the two vectors using the cosine similarity as suggested in [20]. If we denote by A the output of the STA, this angle is given by:

$$E(\bar{K}, A) = cos^{-1} \frac{< \bar{K}, A >}{\|\bar{K}\| \ \|A\|\|}, \tag{1}$$

where $\bar{K}$ is the Ground Truth (GT) (the true neuron's kernel defined by (2), and $\|.\|$ the usual euclidean norm.

3.2 Results

3.2.1 Single cell level

In this section we focus on only one neuron chosen arbitrarily in the population. This neuron was located in $(c_x, c_y) = (4\delta_c, 4\delta_c)$ which is at the intersection of blocks, and with a central variance kernel $\sigma_c = 24\delta_\sigma$. Note that this was chosen to have the most favorable situation for BWN-B32 (as shown later in Fig. 4).

For each of the three stimulus types, we considered ten instances of stimulus to generate rasters, i.e., we have ten trials per stimulus and a total of 30 rasters. Each instance of the stimulus represents 20K images, which generated rasters of 11 minutes long.

Neuron responses for each stimuli are indicated in Tab. 1. As expected, stimuli with larger blocks (BWN-B32 and SWN-B32-S4) induced stronger responses. In addition, note that SWN-B32-S4 generates the strongest response. This fact is relevant because, as shown in [21], the STA error decreases in function with the number of spikes.

Stimulus	# spikes	spike rate
BWN-B32	9108	13.8Hz
BWN-B4	6204	9.4Hz
SWN-B32-S4	9438	14.3Hz

Table 1: Average neuron response to each stimuli across trials, with the number of spikes and the corresponding spike rate.

In Fig. 3(A) we show the spatio-temporal kernels estimated with each stimuli. These results can be compared qualitatively with the ground truth, here represented with a spatial discretization of $4\mu m$). With BWN-B32, the result lacks precision in space. It has strong vertical and horizontal edges corresponding to the block size of the stimuli. The temporal part, however, is properly estimated. With BWN-B4, when the block size is less, the results are very noisy in both space and time, and no relevant information was found. With SWN-B32-S4, the spatial part has the same resolution of the ground truth (by construction), and this method gives a good result too in terms of precision. The main shape is captured even if some weak, noisy patterns remain in the periphery. The temporal part is also accurate, as with BWN-B32. These observations suggest that SWN allows increasing the spatial part of the kernel's spatial resolution with the same stimulation time.

In Fig. 3(B) we show how the error (1) evolves in time for each condition (Criterion 3). Estimates are done at every minute of stimulation time, i.e., at time t, STA is estimated based upon spike obtained in the time window $[0, t]$. The SWN error is always the smallest followed by the BWN-B32 and the BWN-B4. Please note that, even when using the BWN-B32 for an extremely long time, the STA error will not converge to 0, due to the different resolutions between the STA and the GT.

Finally, in Fig. 3(C), we estimate the number of times that the neuron's RF was mapped by the end of each minute of stimulation. With BWN-B4, the RF was never mapped (before 11 minutes). In contrast, the number of times that the RF was mapped with BWN-B32 increases with the stimulation time to reach 100% at seven minutes. With SWN-B32-S4, this number rapidly grows to reach 100% at one minute already.

As a whole, these observations on a single neuron suggest that our approach allows better quality RF estimates and that these estimates need less stimulation time. In the next section, we broaden the scope by considering an entire population of neurons to verify whether these observations hold in general cases.

3.2.2 Population level

Let us consider now the population of 216 neurons defined in Sec. 3.1.3. As in Sec. 3.2.1, the three stimuli were presented for 11 minutes. Note that since inter-trial variability is low (see Fig. 3(B), we use only one trial in this section.

In Fig. 4(A), we show the error between STA and GT (Criterion 3), after 11 minutes, and other the whole population. This compact representation gives very instructive insights into the precision reached by each stimulus and how this performance depends on the neurons' characteristics. First, globally, the average error over all the population is equal to 55.6, 83.6, and 48.7 degrees for BWN-B32, BWN-B4, and SWN-B32-S4, respectively. Then, in more details, starting with BWN-B4, we observe that strong errors are made for most neurons in the population. This observation is related to the slow rate of convergence with this stimulus, as observed in the single neuron case. We note a minor exception for the smallest RF, which seems to be better-captured thanks to the small block sizes. Considering larger block size, namely BWN-B32, we observe that the error decreases as the RFs become larger. This is coherent because block size has to be in some adequation with the RF we want to estimate. Another effect appears, which is some dependence on the neurons' position relative to the block. When neurons' position is "in-between" blocks, then errors become larger. This observation has to be related to some least degree of response since, in some way, neurons in this position will "see" less temporal variations on average. Interestingly, this effect completely disappears with our approach. With SWN-B32-S4, there is still a continuous decrease of error as the RFs become larger, but there is no dependence on the neurons' position. This property will be a strong advantage when dealing with real data since

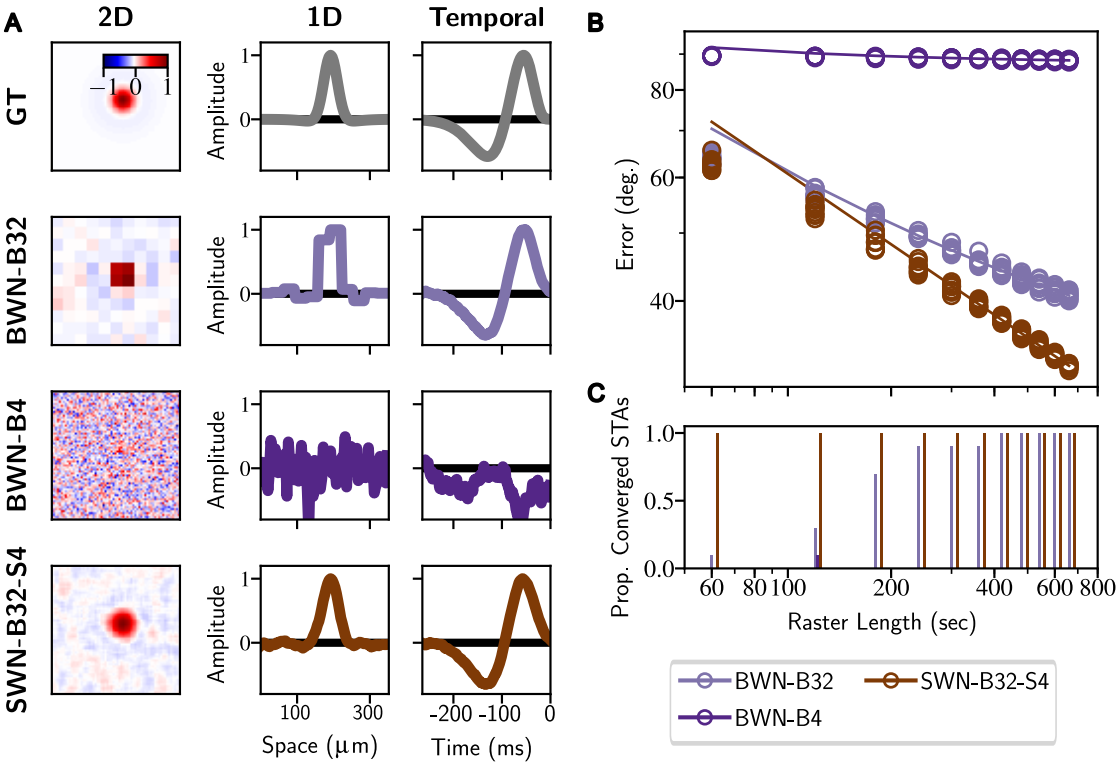

Figure 3: Single neuron analysis. (A) Comparison of spatio-temporal RF estimations. From the 3D point with maximal amplitude in the spatial-temporal RF, the 2D profile is a spatial slice at that point, the 1D profile is the horizontal cut of the 2D profile passing through that point, and finally, the temporal profile is the temporal cut passing through that point. The SWN allows for increasing the spatial part quality while preserving the quality of the temporal profile. (B) Error as a function of time between the RF estimate and GT. An estimate is done at each minute (circles, for each trial) and we fit this error with a power law (continuous line). The SWN always performs better than BWN, and the convergence rate is faster. (C) Proportion of mapped RFs at each minute. It is noticeable that very early, from the first minute, 100% of RF can be mapped with SWN. To reach 100%, one must wait seven minutes with BWN-B32. For BWN-B4, convergence is much slower so that no RF can be fit before 11 minutes.

we do not need to worry about neuron's positions.

In Figs. 4(B)–(C), we consider the parametric evaluation, i.e., we compare the parameters of the fitted kernel with the original ones (Criterion 2). These two figures show kernel parameters at two time instant, five minutes and 11 minutes on the left and right of each figure respectively. They complement the results from Fig. 4(A) in two ways: (1) they provide an interpretation of the nature of the error, and (2) they give an idea of the evolution in time of this error. The following observations can be made. Both BWN-B32 and SWN-B32-S4 resulted in biased fittings, towards a larger center size than the GT's. For the BWN-B32 this bias essentially remains over time, while for SWN-B32-S4 it decreases (Fig. 4(B)). Furthermore, BWN-B32 bias depended on the RF position while, with a longer raster the SWN-B32-S4 bias became independent of the position (Fig. 4(C)). Concerning BWN-B4, there is no bias, at least for the very small RFs that could be mapped. By lack of mapped RFs, no data is available for the medium and large RFs.

4 Testing the approach on real data

4.1 Methods

4.1.1 Simuli

In the experimental analysis we considered four stimuli: two BWNs of low and high resolution (160 µm and 40 µm, respectively) and two SWNs whose STA is of high and super high resolution (for both stimuli blocks of 160 µm and shifts of 40 µm and 4 µm, respectively).

We generated 60K images of each stimulus grouped in 20 blocks of 3000 images. These blocks were randomly sorted before projecting onto the retina to avoid the decrease of neural responses with time aftereffects only one of the stimuli. Each image was 664×664 pixels, where one pixel corresponds to a square of size $4\,\mu\text{m})^2$. Images were refreshed at 30.3Hz meaning, each image was showed for 33 mm.

Light stimuli were projected onto the retina as described previously in [23] and attenuated using neutral density filters to high mesopic light levels (mean luminance 11 cd/m2).

4.1.2 MEA recordings and sorting

All experimental procedures were approved by the ethics committee at Newcastle University and carried out in accordance with the guidelines of the UK Home Office, under control of the Animals (Scientific Procedures) Act 1986. Experiments were performed as described previously in [11].

Briefly, a female mouse (aged P42) was dark adapted overnight and killed by cervical dislocation. Eyes were enucleated, and following removal of the cornea, lens, and vitreous body, they were placed in artificial cerebrospinal fluid (aCSF) containing the following (in mM): 118NaCl, $25NaHCO_3$, $1NaH_2PO_4$, 3KCl, $1MgCl_2$, $2CaCl_2$, 10 glucose, and 0.5 l-Glutamine, equilibrated with 95% O2 and 5% CO2. The retina was isolated from the eye cup and flattened for MEA recordings. All procedures were performed in dim red light, and the room was maintained in darkness throughout the experiment. Retinal recordings were performed on the BioCam4096 platform with BioChips 4096S+ (3Brain GmbH, Lanquart, Switzerland), integrating 4096 square microelectrodes ($21 \times 21\,\mu\text{m}$, pitch 42 µm) on an active area of 2.67×2.67 mm.

The spatial extent (7.12 mm) of the APS-MEA chip allowed us to record simultaneously from large retinal areas (see Fig. 6). The small electrode pitch (42 µm) enables sampling from many individual Retinal Ganglion Cells (RGCs) from these areas, providing us with an unbiased very large analytical sample size. After recording the retinal activity, spikes were sorted and the rasters

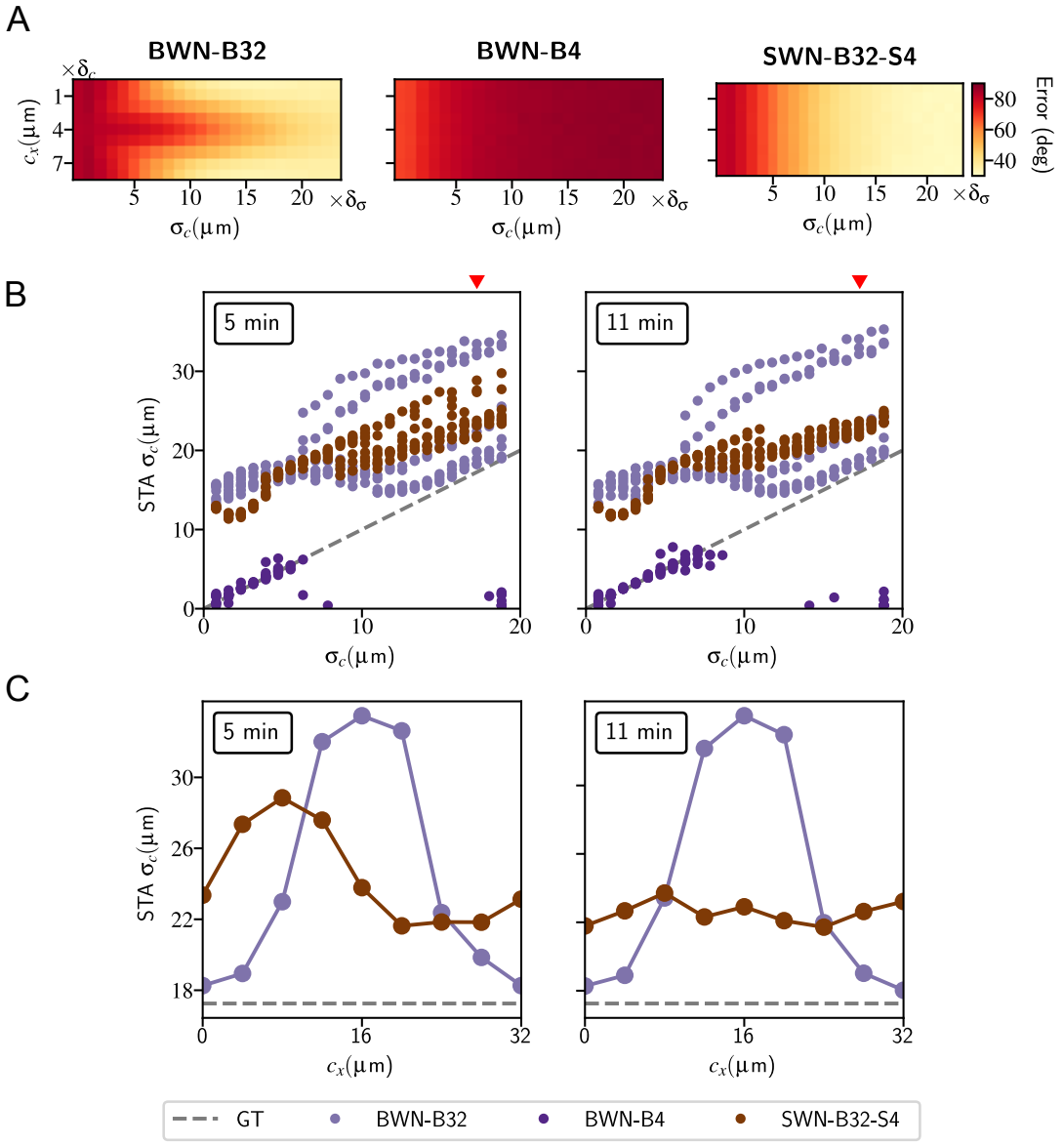

Figure 4: Population analysis. (A) Error between the RF estimate and GT, as a function of position and size. Results show that SWN-B32-S4 offers the best performance at the population level, with no dependence on the neurons' position. (B)–(C) Comparing the fitted kernel parameters with the original ones after five minutes and 11 minutes, respectively. (B) Estimated sizes against the ground truth sizes for all RFs. On the left at five min of stimulation, on the right at 11 min of stimulation. (C) Estimated sizes in function of the RF position for the neurons with $\sigma_c = 17.25$. On the left at five min of stimulation, on the right at 11 min of stimulation. Results show that stimuli with large block sizes give biased RF sized. These biases remain in time but tend to become more uniform with SWN-B32-S4 contrarily to BWN-B32 where they always depend on the neuron's position. With a small block size, i.e., BWN-B32, the situation is different. No bias is observed, but this is only true for a minimal number of neurons for which the RF was mapped.

were formed. Single-unit spikes were sorted using the T-Distribution Expectation-Maximisation algorithm in Offline Sorter (Plexon Inc, Dallas, USA).

4.1.3 STA

Before executing the STA, the stimulus images (independently of the stimulus) were cropped at (640×640) pixels to remove the partial blocks and resized to the smallest size possible without compromising the results. Precisely, the images of BWN-B160 were reduced to (16×16) pixels, BWN-B40 and SWN-B160-S40 were reduced to (40×40) pixels, and SWN-B160-S4 was not resized. This reduction, allowed to reduce the population STA computation time from days to several minutes (in BWN-B160) or hours (BWN-B40 and SWN-B160-S40). The STA estimation was performed as in synthetic data (Section 3.1.4).

4.1.4 Evaluation

All responsive cells were considered for evaluation. First the STA was estimated and analysed using Criterion 1 (Number of mapped RFs). For the neurons whose RF was mapped the Criterion 2 (RF parametric description) was considered. However, for this data, only the center Gaussian was considered, as it is usual in the analysis of mouse retinal RFs [11]. Criteria 3 could not be used since GT was not available.

4.2 Results

4.2.1 Single neuron level

In Fig. 5 we show four representative cases of estimated RFs. For these four neurons, we observe different situations concerning the number of mapped RFs measured with Criteria 1 (Sec. 3.1.5). In all cases selected, SWN-B160-S4 was mapped. No striking difference appear between the SWNs with shifts of 40 µm and 4 µm (when both were mapped). Results with BWN-B40 are always noisy, even when the RF is mapped. Compared to the synthetic case, we also found several analogies. RFs estimated with the SWN stimuli were smoother than RFs estimated with the BWN. The RF temporal profile was not altered by the shifting process.

4.2.2 Neural Population

In Fig. 6(A) we show the log spiking activity of the retina: responses to light occurred across the entire active area of the MEA, with particular emphasis on the dorsal-lateral axis. Due to the strong activity, one can see that the retina was well attached to the MEA array and that the results of the data analysis are reliable and solid.

In Fig. 6(B) we show the distribution of the centers of all mapped RFs depending on the stimulus type. To do so, after fitting STAs with DOGs, we could recess their center position and their size. Overall, the distribution of the STA's center was similar to the activity map for the stimuli BWN-B160 and both SWN. However, when looking closer, RF centers of BWN-B160 tended to be less uniformly distributed, more concentrated, especially on the ventral direction.

In Fig. 7(A)–(B) we analyse STA convergence properties with respect to the four stimuli. In Fig. 7(A), we show a basic count of the number of receptive fields found. The SWNs method over perform the BWNs method in all conditions. Interestingly, we also observe different behaviors if we want to increase the resolution. With BWN, one can increase the resolution by diminishing the block size, but this has a detrimental effect on the number of cells found. With SWN, one can increase the resolution by diminishing the baseline shift, resulting in even more cells found. If we fix the final STA resolution to 40 µm, using the SWN we mapped 19 times more RFs than

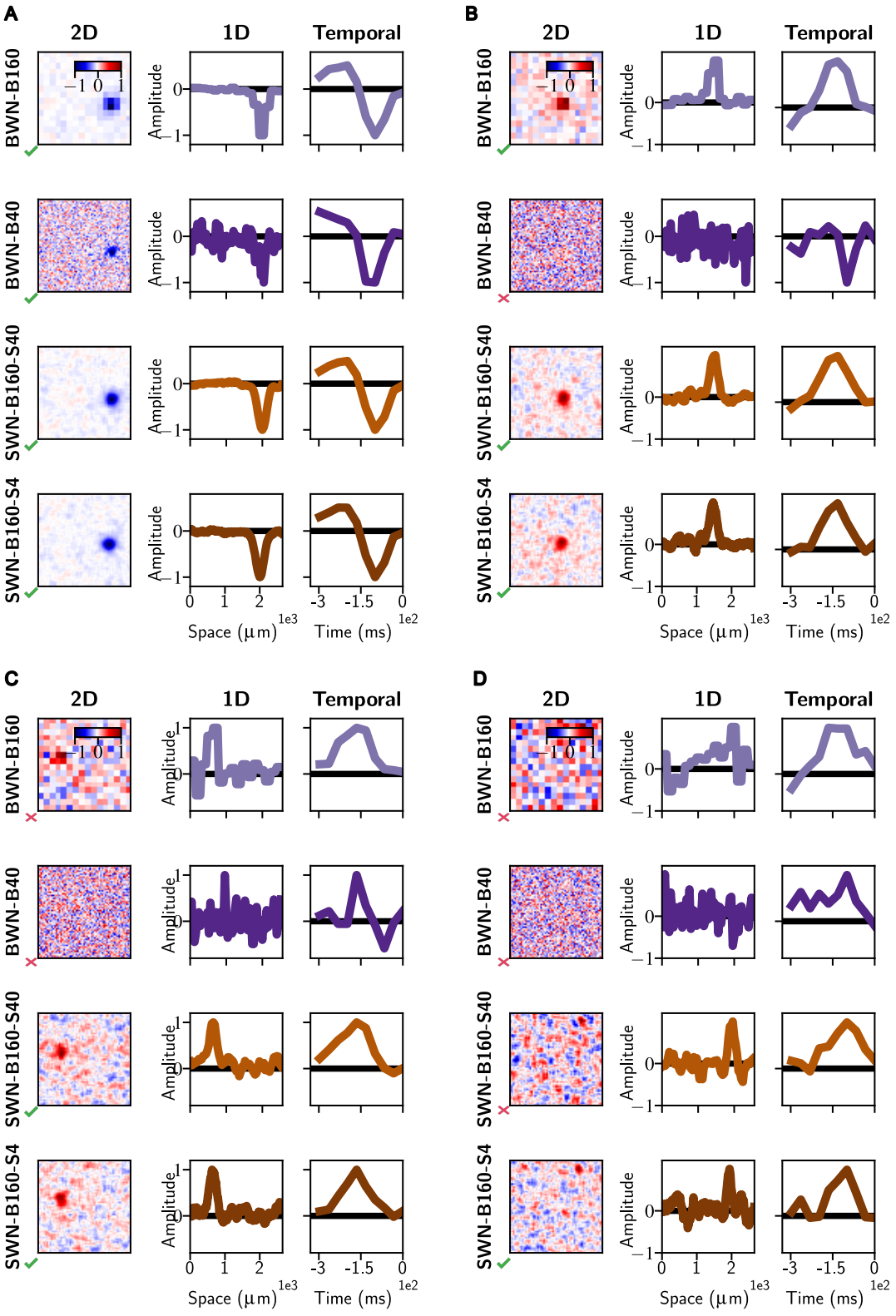

Figure 5: STAs representatives examples for four neurons, showing different situations in terms of RF mapping depending on the stimulus. The representation is the same as in Fig. 3. A green tick icon (resp. a red cross icon) is used to indicate that the RF was mapped or not.

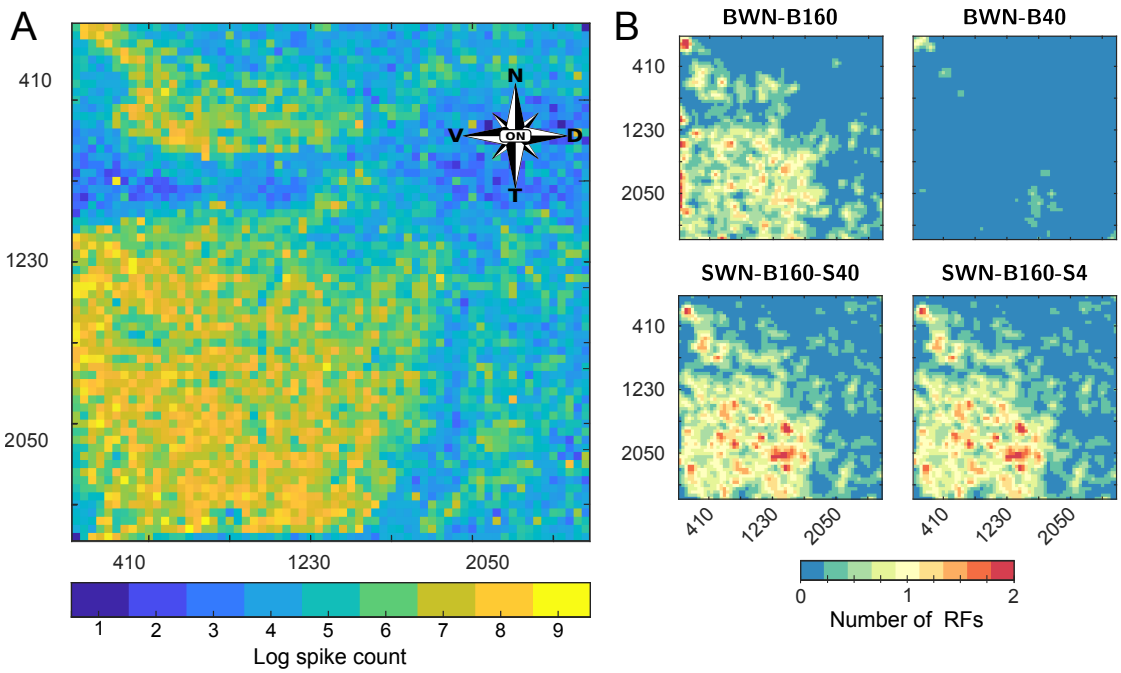

Figure 6: Retinal activity pan-retinal view. (A) The Log spike count during the entire experiment for each retinal channel. This results in a visualisation of the retina outline and gives an overall estimation of the number of active channels. (B) Number of RFs distributed over the MEA. For visualization purposes the values were smoothed with a Gaussian kernel.

using the BWN. A step further, in Fig. 7(B), we look in more details which cells were found with which stimuli. This is represented as an Euler diagram showing percentages of cells. Note that percentages below 2% are not shown. Except for a few cells, we observe the following pattern of inclusions:

$$\text{BWN-B40} \subset \text{BWN-B160} \subset \text{SWN-B160-S40} \subset \text{SWN-B160-S4}.$$

Note that a small RFs' percentage was mapped with SWN-B160-S40 and not with SWN-B160-S4, but this number is four times smaller than the reverse situation.

In Fig. 7(C) we compare the estimated center sizes for the mapped receptive fields. As in the synthetic case, the BWN of high resolution was pruned for small center sizes, while the BWN of low resolution and both SWN were pruned to larger radii. Furthermore, with BWN, the radii distribution is less homogeneous, with higher kurtosis. With SWN, on the other hand, the the radii distribution is more even and covers a broader range of values. This difference in the size's distribution shape means that the SWN could map broader variability of neural preferences than the BWN, which is very desirable when a population of neurons is recorded simultaneously.

5 Discussion and conclusion

In a nutshell, Spike Triggered Average (STA) consists in projecting onto a visual neurons' Receptive Field (RF) white-noise stimuli, here called BWN, and apply a reverse-correlation technique [20, 4, 25, 9]. This approach can be very efficient to estimate isolated neurons' RF since stimulus characteristics, namely the block size, can be adjusted to the targetted neuron. How-

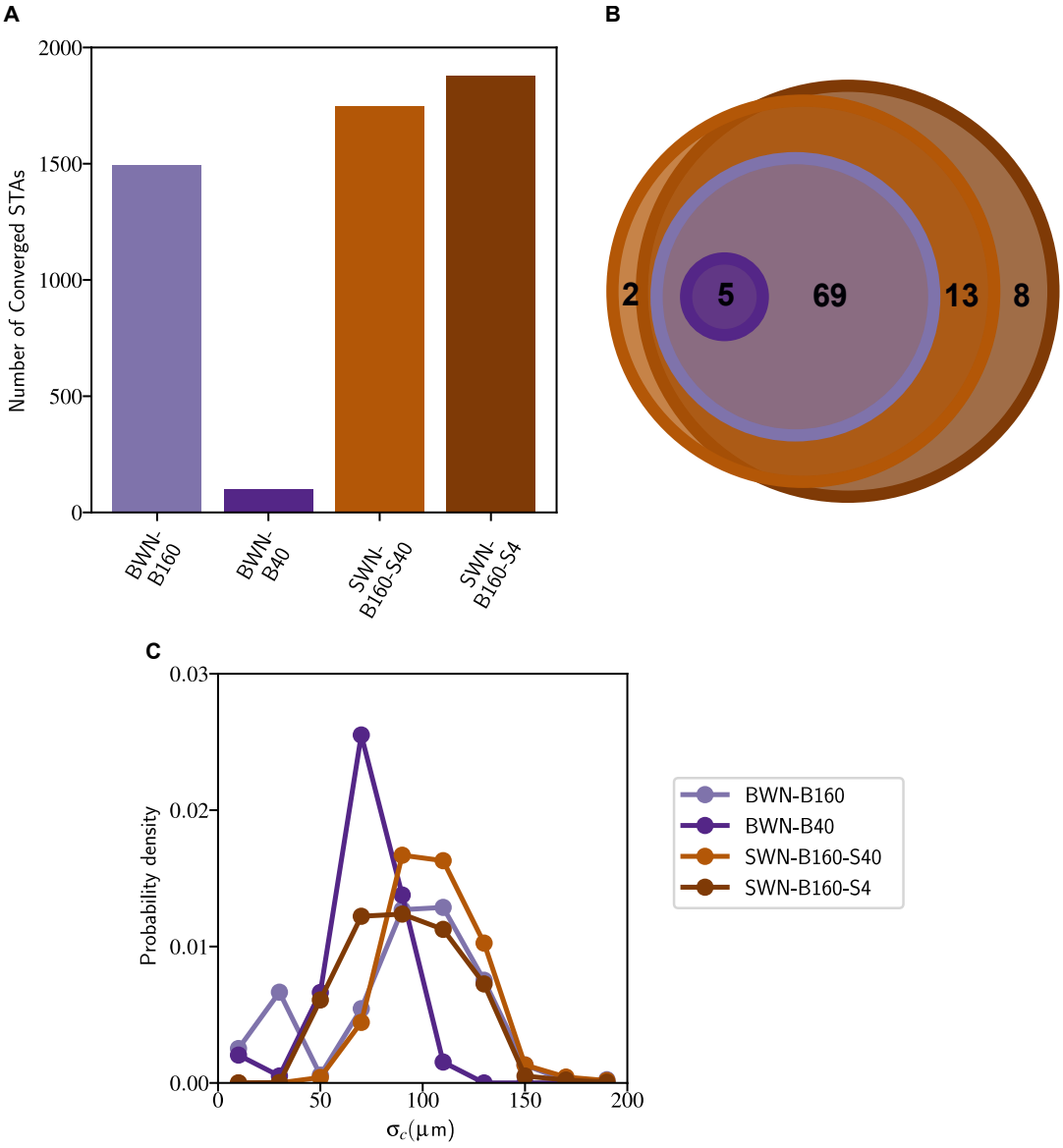

Figure 7: Mapped RFs statistics. (A) Number of mapped RFs per stimulus. (B) Euler diagram (in percentage) of mapped RFs. (C) Distribution of RFs sizes per stimulus.

ever, when applied to a neuron population, such adjustment becomes impossible, and one needs to find some good compromise. If the block size is too small, large receptive fields will likely be missed since neurons will not respond enough. On the contrary, if the block size is too large, small RF will be missed, and the resolution of the RF found will be coarse.

In this paper, we revisited the classical STA approach, having in mind the population case. Instead of searching for optimal block size, we introduced another type of stimuli allowing us to vary the resolution independently of the block size. To do so, we took some inspiration from the computer vision literature, and more particularly from super-resolution techniques. This idea led us to propose a new type of stimuli, directly built from the original white-noise stimuli, but with a significant difference being that random spatial shifts are introduced in time considering a baseline shift. We named these stimuli SWN. Interestingly, the final resolution is now defined by the baseline shift and not anymore by the block size.

Our approach performs better at the single-cell level. As clearly established using a synthetic case, with SWN, RF estimation is independent of the neuron's position relative to the stimulus (not the case for the BWN). The resolution always tends to be better with SWN, since there is no compromise between responsiveness and resolution. Here, we increase the resolution by diminishing the baseline shift of the stimuli.

Our approach is stronger at the population-level. Not only we get RF with better resolution, but also we get more RF, with more neuronal variability. This property also results from the construction of the SWN stimuli: given block size, even if this block size is not optimal for some cells, the fact of introducing more variability through the random shifts make neurons more responsive, which is essential for the STA approach.

Our approach maps faster RFs. This property results directly from the neurons' increased activity, which makes the STA approach more efficient. In the synthetic case, we showed that the whole population could be mapped seven times faster with SWN. This is relevant because STA is often a preliminary step of analysis in an experimental set up (see, e.g., [23]). Therefore, one cannot generate long rasters to map RFs. Our approach allows to map more neurons with shorter stimulation times.

All these properties bring substantial advantages for experimentalists [11]. With SWN, since convergence is faster than with BWN, less time needs to be allocated to STA (and thus more time is available for the experiment), more cells are found, and RF resolution is even faster. The new stimuli are also easy to produce[2] and the same reverse correlation methods can be used to recover the RF. Of course, in practice, one still needs to choose a suitable block size. This choice still relies on the experimenter expertise, but with SWN, it is less critical since the variability introduced by the shift will compensate for a sub-optimal block size value. A possible strategy is to start adjusting the block size with BWN prior to the experiment and then set the baseline shift according to the desired resolution.

Computationally, we found that the STA mapped with the SWN are larger than the ground truth, but this bias seems to decrease with stimulation time. In contrast, similar bias was found in the low resolution BWN, but not changing significantly with time. For the experimental data here tested, we founded that the resolution of 4 µm, meaning one pixel, increased the computing costs (both execution time and memory space) but did not boost the general results. However, on different experimental set-ups, for instance, recordings from animals with smaller RFs, an extremely high resolution might be of great interest.

The general approach applied to STA in this paper — making use of super-resolution methods to boost the performance of RF estimation methods — will allow for more efficient stimuli design. In particular, a similar idea could be applied in the temporal domain by randomizing each frame's presentation time in the stimulus. We also expect that this general approach could be applicable

[2]Python code with representative examples will be provided upon acceptance of the paper.

to other spike-triggered methods like the Spike Triggered Covariance [20, 26], since it is a good approximation of Gaussian White Noise, spherical and easy to implement.

References

[1] Atencio, C.A., Sharpee, T.O., Schreiner, C.E.: Cooperative nonlinearities in auditory cortical neurons. Neuron **58**(6), 956–966 (2008)

[2] Berdondini, L., Imfeld, K., Maccione, A., Tedesco, M., Neukom, S., Koudelka-Hep, M., Martinoia, S.: Active pixel sensor array for high spatio-temporal resolution electrophysiological recordings from single cell to large scale neuronal networks. Lab on a Chip **9**(18), 2644–2651 (2009)

[3] Cessac, B., Kornprobst, P., Kraria, S., Nasser, H., Pamplona, D., Portelli, G., Viéville, T.: Pranas: A new platform for retinal analysis and simulation. Frontiers in Neuroinformatics **11**, 49 (2017). DOI 10.3389/fninf.2017.00049. URL `http://journal.frontiersin.org/article/10.3389/fninf.2017.00049`

[4] Chichilnisky, E.J.: A simple white noise analysis of neuronal light responses. Network: Comput. Neural Syst. **12**, 199–213 (2001)

[5] Croner, L.J., Kaplan, E.: Receptive fields of P and M ganglion cells across the primate retina. Vision research **35**(1), 7–24 (1995)

[6] Dayan, P., Abbott, L.F.: Theoretical neuroscience: computational and mathematical modeling of neural systems. Computational Neuroscience Series (2001)

[7] DeAngelis, G.C., Ohzawa, I., Freeman, R.D.: Spatiotemporal organization of simple-cell receptive fields in the cat's striate cortex. i. general characteristics and postnatal development. Journal of neurophysiology **69**(4), 1091–1117 (1993)

[8] Földiák, P.: Stimulus optimisation in primary visual cortex. Neurocomputing **38-40**, 1217–1222 (2001)

[9] Gollisch, T.: Estimating receptive fields in the presence of spike-time jitter. Network: Computation in Neural Systems **17**(2), 103–129 (2006)

[10] Greenspan, H.: Super-resolution in medical imaging. Computer Journal **52**(1), 43–63 (2009). DOI 10.1093/comjnl/bxm075

[11] Hilgen, G., Pirmoradian, S., Pamplona, D., Kornprobst, P., Cessac, B., Hennig, M.H., Sernagor, E.: Pan-retinal characterization of light responses from ganglion cells in the developing mouse retina. bioRxiv (2016)

[12] Jones, J.P., Palmer, L.A.: The two-dimensional spatial structure of simple receptive fields in cat striate cortex. Journal of Neurophysiology **58**(6), 1187–1211 (1987)

[13] Liu, C., Sun, D.: A bayesian approach to adaptive video super resolution. In: IEEE Computer Society Conference on Computer Vision and Pattern Recognition (CVPR), pp. 209–216 (2011)

[14] Machens, C.K.: Adaptive sampling by information maximization. Physical review letters **88**(2), 228104 (2002)

[15] MacKay, D.J.C.: Information-based objective functions for active data selection. Neural Computation **4**, 590–604 (1992)

[16] The Mathworks, Inc., Natick, Massachusetts: MATLAB version 9.3.0.713579 (R2017b) (2017)

[17] Merino, M.T., Nunez, J.: Super-resolution of remotely sensed images with variable-pixel linear reconstruction. IEEE Transactions on Geoscience and Remote Sensing **45**(5), 1446–1457 (2007)

[18] Moré, J.J., Sorensen, D.C.: Computing a trust region step. SIAM Journal on Scientific and Statistical Computing **4**(3), 553–572 (1983)

[19] Odermatt, B., Nikolaev, A., Lagnado, L.: Encoding of luminance and contrast by linear and nonlinear synapses in the retina. Neuron **73**(4), 758–773 (2012)

[20] Paninski, L.: Convergence properties of three spike-triggered analysis techniques. Network **14**, 437–464 (2003)

[21] Paninski, L.: Maximum likelihood estimation of cascade point-process neural encoding models. Network: Comput. Neural Syst. **15**(04), 243–262 (2004)

[22] Peeters, R.R., Kornprobst, P., Nikolova, M., Sunaert, S., Vieville, T., Malandain, G., Deriche, R., Faugeras, O., Ng, M., Van Hecke, P.: The use of super-resolution techniques to reduce slice thickness in functional mri. International Journal of Imaging Systems and Technology **14**(3), 131–138 (2004)

[23] Portelli, G., Barrett, J.M., Hilgen, G., Masquelier, T., Maccione, A., Di Marco, S., Berdondini, L., Kornprobst, P., Sernagor, E.: Rank order coding: a retinal information decoding strategy revealed by large-scale multielectrode array retinal recordings. eNeuro **3**(3) (2016)

[24] Rodieck, R.W.: Quantitive analysis of cat retinal ganglion cell response to visual stimuli. Vision Research **5**(12), 583–601 (1965)

[25] Schwartz, O., Pillow, J.W., Rust, N.C., Simoncelli, E.P.: Spike-triggered neural characterization. Journal of vision **6**, 484–507 (2006)

[26] Simoncelli, E.P., Paninski, J.P., Pillow, J., Schwartz, O.: Characterization of neural responses with stochastic stimuli. The cognitive neurosciences, 3rd edition pp. 327–338 (2004)

[27] Wang, H., Wen, D.: The progress of sub-pixel imaging methods. In: J. Ojeda-Castaneda, S. Han, P. Jia, J. Fang, D. Fan, L. Qian, Y. Gu, X. Yan (eds.) Selected Papers from Conferences of the Photoelectronic Technology Committee of the Chinese Society of Astronautics: Optical Imaging, Remote Sensing, and Laser-Matter Interaction 2013, vol. 9142, pp. 166–170. International Society for Optics and Photonics, SPIE (2014)

[28] Yue, L., Shen, H., Li, J., Yuan, Q., Zhang, H., Zhang, L.: Image super-resolution: The techniques, applications, and future. Signal Processing **128**, 389–408 (2016)

6 Supplementary material

6.1 LPN neuron model

The Linear-Nonlinear Poisson (LNP) model used in the simulation part (see Sec. 3) has three stages:

Stage 1 describes how the neuron integrates stimulus intensity over space and time. The stimulus is denoted by $S(x, y, t)$ where $(x, y) \in \{0 \dots M, 0 \dots N\}$ and $t \in \{0, 1, 2, \dots\}$. The spatio-temporal kernel of the neuron is denoted by $K(x, y, t)$ where $(x, y) \in \{0 \dots M, 0 \dots N\}$ and $t \in \{0, \dots, T\}$ (i.e., T is its temporal support) The resulting integration denoted by $L(t)$ is defined by an inner product in space and a convolution in time:

$$L(t) = \sum_{\tau=0}^{T} \sum_{x=0}^{N} \sum_{y=0}^{M} K(x, y, \tau) S(x, y, t - \tau).$$

Then we assume that the kernel K is separable is space and time, i.e.:

$$K(x, y, t) = K_S(x, y) K_T(t), \tag{2}$$

where each part of the kernel is defined according to classical models of retinal processing [5, 24], namely DOG for the spatial part and a polynomial multiplied by a decaying exponential for the temporal part:

$$\begin{aligned} K_S(x, y) =& 16 \frac{1}{2\pi\sigma_c^2} \exp\left(-\frac{1}{2\sigma_c^2}\left((x - x_x)^2 + (y - x_y)^2\right)\right) \\ &- 8 \frac{1}{2\pi\sigma_s^2} \exp\left(-\frac{1}{2\sigma_s^2}\left((x - c_x)^2 + (y - c_y)^2\right)\right), \\ K_T(t) =& \left(-\frac{(0.7t)^7}{7!} + \frac{(0.7t)^5}{5!}\right) \exp\left(-0.7t\right), \end{aligned} \tag{3}$$

where parameters σ_c, σ_s define the spatial integration properties of the neuron (for center and surround) and (c_x, c_y) is the position of its center. These are the parameters that we vary to define the population.

Stage 2 gives the instantaneous spike rate $\lambda(t)$ by passing the output of the first stage by a non linearity:

$$\lambda(t) = f(L(t)), \text{ where } f(L) = \frac{1}{1 + \exp\left(-0.05L - 100\right)}.$$

Stage 3 converts the spike rate into a series of spikes using an inhomogeneous Poisson process. The time of the spikes is discretized into time bins of $1ms$.

Contents

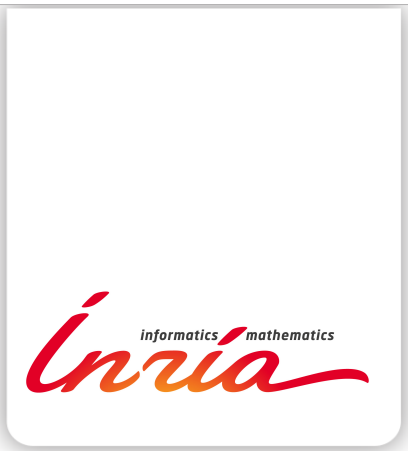

RESEARCH CENTRE
SOPHIA ANTIPOLIS – MÉDITERRANÉE

2004 route des Lucioles - BP 93
06902 Sophia Antipolis Cedex

Publisher
Inria
Domaine de Voluceau - Rocquencourt
BP 105 - 78153 Le Chesnay Cedex
inria.fr

ISSN 0249-6399